Update of the search for supersymmetric particles in scenarios with Gravitino LSP and Sleptons NLSP

DELPHI Collaboration

Abstract

An update of the search for sleptons, neutralinos and charginos in the context of scenarios where the lightest supersymmetric particle is the gravitino and the next-to-lightest supersymmetric particle is a slepton, is presented, together with the update of the search for heavy stable charged particles in light gravitino scenarios and Minimal Supersymmetric Standard Models. Data collected in 1999 with the DELPHI detector at centre-of-mass energies around 192, 196, 200 and 202 GeV were analysed. No evidence for the production of these supersymmetric particles was found. Hence, new mass limits were derived at 95% confidence level.

arXiv:hep-ex/0102038v1 20 Feb 2001

P.Abreu[23], W.Adam[52], T.Adye[38], P.Adzic[12], Z.Albrecht[19], T.Alderweireld[2], G.D.Alekseev[18], R.Alemany[9], T.Allmendinger[19], P.P.Allport[24], S.Almehed[26], U.Amaldi[30], N.Amapane[47], S.Amato[49], E.Anashkin[37], E.G.Anassontzis[3], P.Andersson[46], A.Andreazza[29], S.Andringa[23], N.Anjos[23], P.Antilogus[27], W-D.Apel[19], Y.Arnoud[16], B.Åsman[46], J-E.Augustin[25], A.Augustinus[9], P.Baillon[9], A.Ballestrero[47], P.Bambade[9,21], F.Barao[23], G.Barbiellini[48], R.Barbier[27], D.Y.Bardin[18], G.Barker[19], A.Baroncelli[40], M.Battaglia[17], M.Baubillier[25], K-H.Becks[54], M.Begalli[6], A.Behrmann[54], Yu.Belokopytov[9], K.Belous[44], N.C.Benekos[33], A.C.Benvenuti[5], C.Berat[16], M.Berggren[25], L.Berntzon[46], D.Bertrand[2], M.Besancon[41], N.Besson[41], M.S.Bilenky[18], D.Bloch[10], H.M.Blom[32], L.Bol[19], M.Bonesini[30], M.Boonekamp[41], P.S.L.Booth[24], G.Borisov[21], C.Bosio[43], O.Botner[50], E.Boudinov[32], B.Bouquet[21], T.J.V.Bowcock[24], I.Boyko[18], I.Bozovic[12], M.Bozzo[15], M.Bracko[45], P.Branchini[40], R.A.Brenner[50], P.Bruckman[9], J-M.Brunet[8], L.Bugge[34], P.Buschmann[54], M.Caccia[29], M.Calvi[30], T.Camporesi[9], V.Canale[39], F.Carena[9], L.Carroll[24], C.Caso[15], M.V.Castillo Gimenez[51], A.Cattai[9], F.R.Cavallo[5], M.Chapkin[44], Ph.Charpentier[9], P.Checchia[37], G.A.Chelkov[18], R.Chierici[47], P.Chliapnikov[9,44], P.Chochula[7], V.Chorowicz[27], J.Chudoba[31], K.Cieslik[20], P.Collins[9], R.Contri[15], E.Cortina[51], G.Cosme[21], F.Cossutti[9], M.Costa[51], H.B.Crawley[1], D.Crennell[38], J.Croix[10], J.Cuevas Maestro[35], S.Czellar[17], J.D'Hondt[2], J.Dalmau[46], M.Davenport[9], W.Da Silva[25], G.Della Ricca[48], P.Delpierre[28], N.Demaria[47], A.De Angelis[48], W.De Boer[19], C.De Clercq[2], B.De Lotto[48], A.De Min[9], L.De Paula[49], H.Dijkstra[9], L.Di Ciaccio[39], K.Doroba[53], M.Dracos[10], J.Drees[54], M.Dris[33], G.Eigen[4], T.Ekelof[50], M.Ellert[50], M.Elsing[9], J-P.Engel[10], M.Espirito Santo[9], G.Fanourakis[12], D.Fassouliotis[12], M.Feindt[19], J.Fernandez[42], A.Ferrer[51], E.Ferrer-Ribas[21], F.Ferro[15], A.Firestone[1], U.Flagmeyer[54], H.Foeth[9], E.Fokitis[33], F.Fontanelli[15], B.Franek[38], A.G.Frodesen[4], R.Fruhwirth[52], F.Fulda-Quenzer[21], J.Fuster[51], A.Galloni[24], D.Gamba[47], S.Gamblin[21], M.Gandelman[49], C.Garcia[51], C.Gaspar[9], M.Gaspar[49], U.Gasparini[37], Ph.Gavillet[9], E.N.Gazis[33], D.Gele[10], T.Geralis[12], N.Ghodbane[27], I.Gil[51], F.Glege[54], R.Gokieli[9,53], B.Golob[9,45], G.Gomez-Ceballos[42], P.Goncalves[23], I.Gonzalez Caballero[42], G.Gopal[38], L.Gorn[1], Yu.Gouz[44], V.Gracco[15], J.Grahl[1], E.Graziani[40], G.Grosdidier[21], K.Grzelak[53], J.Guy[38], C.Haag[19], F.Hahn[9], S.Hahn[54], S.Haider[9], A.Hallgren[50], K.Hamacher[54], J.Hansen[34], F.J.Harris[36], S.Haug[34], F.Hauler[19], V.Hedberg[9,26], S.Heising[19], J.J.Hernandez[51], P.Herquet[2], H.Herr[9], O.Hertz[19], E.Higon[51], S-O.Holmgren[46], P.J.Holt[36], S.Hoorelbeke[2], M.Houlden[24], J.Hrubec[52], G.J.Hughes[24], K.Hultqvist[9,46], J.N.Jackson[24], R.Jacobsson[9], P.Jalocha[20], Ch.Jarlskog[26], G.Jarlskog[26], P.Jarry[41], B.Jean-Marie[21], D.Jeans[36], E.K.Johansson[46], P.Jonsson[27], C.Joram[9], P.Juillot[10], L.Jungermann[19], F.Kapusta[25], K.Karafasoulis[12], S.Katsanevas[27], E.C.Katsoufis[33], R.Keranen[19], G.Kernel[45], B.P.Kersevan[45], Yu.Khokhlov[44], B.A.Khomenko[18], N.N.Khovanski[18], A.Kiiskinen[17], B.King[24], A.Kinvig[24], N.J.Kjaer[9], O.Klapp[54], P.Kluit[32], P.Kokkinias[12], V.Kostioukhine[44], C.Kourkoumelis[3], O.Kouznetsov[18], M.Krammer[52], E.Kriznic[45], Z.Krumstein[18], P.Kubinec[7], M.Kucharczyk[20], J.Kurowska[53], J.W.Lamsa[1], J-P.Laugier[41], G.Leder[52], F.Ledroit[16], L.Leinonen[46], A.Leisos[12], R.Leitner[31], G.Lenzen[54], V.Lepeltier[21], T.Lesiak[20], M.Lethuillier[27], J.Libby[36], W.Liebig[54], D.Liko[9], A.Lipniacka[46], I.Lippi[37], J.G.Loken[36], J.H.Lopes[49], J.M.Lopez[42], R.Lopez-Fernandez[16], D.Loukas[12], P.Lutz[41], L.Lyons[36], J.MacNaughton[52], J.R.Mahon[6], A.Maio[23], A.Malek[54], S.Maltezos[33], V.Malychev[18], F.Mandl[52], J.Marco[42], R.Marco[42], B.Marechal[49], M.Margoni[37], J-C.Marin[9], C.Mariotti[9], A.Markou[12], C.Martinez-Rivero[9], S.Marti i Garcia[9], J.Masik[13], N.Mastroyiannopoulos[12], F.Matorras[42], C.Matteuzzi[30], G.Matthiae[39], F.Mazzucato[37,14], M.Mazzucato[37], M.Mc Cubbin[24], R.Mc Kay[1], R.Mc Nulty[24], G.Mc Pherson[24], E.Merle[16], C.Meroni[29], W.T.Meyer[1], E.Migliore[9], L.Mirabito[27], W.A.Mitaroff[52], U.Mjoernmark[26], T.Moa[46], M.Moch[19], K.Moenig[9,11], M.R.Monge[15], J.Montenegro[32], D.Moraes[49], P.Morettini[15], G.Morton[36], U.Mueller[54], K.Muenich[54], M.Mulders[32], L.M.Mundim[6], W.J.Murray[38], B.Muryn[20], G.Myatt[36], T.Myklebust[34], M.Nassiakou[12], F.L.Navarria[5], K.Nawrocki[53], P.Negri[30], S.Nemecek[13], N.Neufeld[52], R.Nicolaidou[41], P.Niezurawski[53], M.Nikolenko[10,18], V.Nomokonov[17], A.Nygren[26], V.Obraztsov[44], A.G.Olshevski[18], A.Onofre[23], R.Orava[17], K.Osterberg[9], A.Ouraou[41], A.Oyanguren[51], M.Paganoni[30], S.Paiano[5], R.Pain[25], R.Paiva[23], J.Palacios[36], H.Palka[20], Th.D.Papadopoulou[33], L.Pape[9], C.Parkes[9], F.Parodi[15], U.Parzefall[24], A.Passeri[40], O.Passon[54], L.Peralta[23], V.Perepelitsa[51], M.Pernicka[52], A.Perrotta[5], C.Petridou[48], A.Petrolini[15], H.T.Phillips[38], F.Pierre[41], M.Pimenta[23], E.Piotto[29], T.Podobnik[45], V.Poireau[41], M.E.Pol[6], G.Polok[20], P.Poropat[48], V.Pozdniakov[18], P.Privitera[39], N.Pukhaeva[18], A.Pullia[30], D.Radojicic[36], S.Ragazzi[30], H.Rahmani[33], A.L.Read[34], P.Rebecchi[9], N.G.Redaelli[30], M.Regler[52], J.Rehn[19], D.Reid[32], R.Reinhardt[54], P.B.Renton[36], L.K.Resvanis[3], F.Richard[21], J.Ridky[13], G.Rinaudo[47], I.Ripp-Baudot[10], A.Romero[47], P.Ronchese[37], E.I.Rosenberg[1], P.Rosinsky[7], T.Rovelli[5], V.Ruhlmann-Kleider[41], A.Ruiz[42], H.Saarikko[17], Y.Sacquin[41], A.Sadovsky[18], G.Sajot[16], L.Salmi[17], J.Salt[51], D.Sampsonidis[12], M.Sannino[15], A.Savoy-Navarro[25], C.Schwanda[52], Ph.Schwemling[25], B.Schwering[54], U.Schwickerath[19], F.Scuri[48], P.Seager[22], Y.Sedykh[18], A.M.Segar[36], R.Sekulin[38], G.Sette[15], R.C.Shellard[6], M.Siebel[54], L.Simard[41], F.Simonetto[37], A.N.Sisakian[18], G.Smadja[27], N.Smirnov[44], O.Smirnova[26], G.R.Smith[38], A.Sokolov[44], A.Sopczak[19], R.Sosnowski[53], T.Spassov[9], E.Spiriti[40], S.Squarcia[15], C.Stanescu[40], M.Stanitzki[19], K.Stevenson[36], A.Stocchi[21], J.Strauss[52], R.Strub[10], B.Stugu[4], M.Szczekowski[53], M.Szeptycka[53], T.Tabarelli[30], A.Taffard[24], O.Tchikilev[44], F.Tegenfeldt[50], F.Terranova[30], J.Timmermans[32], N.Tinti[5], L.G.Tkatchev[18],

M.Tobin[24], S.Todorova[9], B.Tome[23], A.Tonazzo[9], L.Tortora[40], P.Tortosa[51], D.Treille[9], G.Tristram[8], M.Trochimczuk[53], C.Troncon[29], M-L.Turluer[41], I.A.Tyapkin[18], P.Tyapkin[26], S.Tzamarias[12], O.Ullaland[9], V.Uvarov[44], G.Valenti[9,5], E.Vallazza[48], C.Vander Velde[2], P.Van Dam[32], W.Van den Boeck[2], J.Van Eldik[9,32], A.Van Lysebetten[2], N.van Remortel[2], I.Van Vulpen[32], G.Vegni[29], L.Ventura[37], W.Venus[38,9], F.Verbeure[2], P.Verdier[27], M.Verlato[37], L.S.Vertogradov[18], V.Verzi[29], D.Vilanova[41], L.Vitale[48], E.Vlasov[44], A.S.Vodopyanov[18], G.Voulgaris[3], V.Vrba[13], H.Wahlen[54], A.J.Washbrook[24], C.Weiser[9], D.Wicke[9], J.H.Wickens[2], G.R.Wilkinson[36], M.Winter[10], M.Witek[20], G.Wolf[9], J.Yi[1], O.Yushchenko[44], A.Zalewska[20], P.Zalewski[53], D.Zavrtanik[45], E.Zevgolatakos[12], N.I.Zimin[18,26], A.Zintchenko[18], Ph.Zoller[10], G.Zumerle[37], M.Zupan[12]

[1]Department of Physics and Astronomy, Iowa State University, Ames IA 50011-3160, USA
[2]Physics Department, Univ. Instelling Antwerpen, Universiteitsplein 1, B-2610 Antwerpen, Belgium
 and IIHE, ULB-VUB, Pleinlaan 2, B-1050 Brussels, Belgium
 and Faculté des Sciences, Univ. de l'Etat Mons, Av. Maistriau 19, B-7000 Mons, Belgium
[3]Physics Laboratory, University of Athens, Solonos Str. 104, GR-10680 Athens, Greece
[4]Department of Physics, University of Bergen, Allégaten 55, NO-5007 Bergen, Norway
[5]Dipartimento di Fisica, Università di Bologna and INFN, Via Irnerio 46, IT-40126 Bologna, Italy
[6]Centro Brasileiro de Pesquisas Físicas, rua Xavier Sigaud 150, BR-22290 Rio de Janeiro, Brazil
 and Depto. de Física, Pont. Univ. Católica, C.P. 38071 BR-22453 Rio de Janeiro, Brazil
 and Inst. de Física, Univ. Estadual do Rio de Janeiro, rua São Francisco Xavier 524, Rio de Janeiro, Brazil
[7]Comenius University, Faculty of Mathematics and Physics, Mlynska Dolina, SK-84215 Bratislava, Slovakia
[8]Collège de France, Lab. de Physique Corpusculaire, IN2P3-CNRS, FR-75231 Paris Cedex 05, France
[9]CERN, CH-1211 Geneva 23, Switzerland
[10]Institut de Recherches Subatomiques, IN2P3 - CNRS/ULP - BP20, FR-67037 Strasbourg Cedex, France
[11]Now at DESY-Zeuthen, Platanenallee 6, D-15735 Zeuthen, Germany
[12]Institute of Nuclear Physics, N.C.S.R. Demokritos, P.O. Box 60228, GR-15310 Athens, Greece
[13]FZU, Inst. of Phys. of the C.A.S. High Energy Physics Division, Na Slovance 2, CZ-180 40, Praha 8, Czech Republic
[14]Currently at DPNC, University of Geneva, Quai Ernest-Ansermet 24, CH-1211, Geneva, Switzerland
[15]Dipartimento di Fisica, Università di Genova and INFN, Via Dodecaneso 33, IT-16146 Genova, Italy
[16]Institut des Sciences Nucléaires, IN2P3-CNRS, Université de Grenoble 1, FR-38026 Grenoble Cedex, France
[17]Helsinki Institute of Physics, HIP, P.O. Box 9, FI-00014 Helsinki, Finland
[18]Joint Institute for Nuclear Research, Dubna, Head Post Office, P.O. Box 79, RU-101 000 Moscow, Russian Federation
[19]Institut für Experimentelle Kernphysik, Universität Karlsruhe, Postfach 6980, DE-76128 Karlsruhe, Germany
[20]Institute of Nuclear Physics and University of Mining and Metalurgy, Ul. Kawiory 26a, PL-30055 Krakow, Poland
[21]Université de Paris-Sud, Lab. de l'Accélérateur Linéaire, IN2P3-CNRS, Bât. 200, FR-91405 Orsay Cedex, France
[22]School of Physics and Chemistry, University of Lancaster, Lancaster LA1 4YB, UK
[23]LIP, IST, FCUL - Av. Elias Garcia, 14-1º, PT-1000 Lisboa Codex, Portugal
[24]Department of Physics, University of Liverpool, P.O. Box 147, Liverpool L69 3BX, UK
[25]LPNHE, IN2P3-CNRS, Univ. Paris VI et VII, Tour 33 (RdC), 4 place Jussieu, FR-75252 Paris Cedex 05, France
[26]Department of Physics, University of Lund, Sölvegatan 14, SE-223 63 Lund, Sweden
[27]Université Claude Bernard de Lyon, IPNL, IN2P3-CNRS, FR-69622 Villeurbanne Cedex, France
[28]Univ. d'Aix - Marseille II - CPP, IN2P3-CNRS, FR-13288 Marseille Cedex 09, France
[29]Dipartimento di Fisica, Università di Milano and INFN-MILANO, Via Celoria 16, IT-20133 Milan, Italy
[30]Dipartimento di Fisica, Univ. di Milano-Bicocca and INFN-MILANO, Piazza delle Scienze 2, IT-20126 Milan, Italy
[31]IPNP of MFF, Charles Univ., Areal MFF, V Holesovickach 2, CZ-180 00, Praha 8, Czech Republic
[32]NIKHEF, Postbus 41882, NL-1009 DB Amsterdam, The Netherlands
[33]National Technical University, Physics Department, Zografou Campus, GR-15773 Athens, Greece
[34]Physics Department, University of Oslo, Blindern, NO-1000 Oslo 3, Norway
[35]Dpto. Fisica, Univ. Oviedo, Avda. Calvo Sotelo s/n, ES-33007 Oviedo, Spain
[36]Department of Physics, University of Oxford, Keble Road, Oxford OX1 3RH, UK
[37]Dipartimento di Fisica, Università di Padova and INFN, Via Marzolo 8, IT-35131 Padua, Italy
[38]Rutherford Appleton Laboratory, Chilton, Didcot OX11 OQX, UK
[39]Dipartimento di Fisica, Università di Roma II and INFN, Tor Vergata, IT-00173 Rome, Italy
[40]Dipartimento di Fisica, Università di Roma III and INFN, Via della Vasca Navale 84, IT-00146 Rome, Italy
[41]DAPNIA/Service de Physique des Particules, CEA-Saclay, FR-91191 Gif-sur-Yvette Cedex, France
[42]Instituto de Fisica de Cantabria (CSIC-UC), Avda. los Castros s/n, ES-39006 Santander, Spain
[43]Dipartimento di Fisica, Università degli Studi di Roma La Sapienza, Piazzale Aldo Moro 2, IT-00185 Rome, Italy
[44]Inst. for High Energy Physics, Serpukov P.O. Box 35, Protvino, (Moscow Region), Russian Federation
[45]J. Stefan Institute, Jamova 39, SI-1000 Ljubljana, Slovenia and Laboratory for Astroparticle Physics,
 Nova Gorica Polytechnic, Kostanjeviska 16a, SI-5000 Nova Gorica, Slovenia,
 and Department of Physics, University of Ljubljana, SI-1000 Ljubljana, Slovenia
[46]Fysikum, Stockholm University, Box 6730, SE-113 85 Stockholm, Sweden
[47]Dipartimento di Fisica Sperimentale, Università di Torino and INFN, Via P. Giuria 1, IT-10125 Turin, Italy
[48]Dipartimento di Fisica, Università di Trieste and INFN, Via A. Valerio 2, IT-34127 Trieste, Italy
 and Istituto di Fisica, Università di Udine, IT-33100 Udine, Italy
[49]Univ. Federal do Rio de Janeiro, C.P. 68528 Cidade Univ., Ilha do Fundão BR-21945-970 Rio de Janeiro, Brazil
[50]Department of Radiation Sciences, University of Uppsala, P.O. Box 535, SE-751 21 Uppsala, Sweden
[51]IFIC, Valencia-CSIC, and D.F.A.M.N., U. de Valencia, Avda. Dr. Moliner 50, ES-46100 Burjassot (Valencia), Spain
[52]Institut für Hochenergiephysik, Österr. Akad. d. Wissensch., Nikolsdorfergasse 18, AT-1050 Vienna, Austria
[53]Inst. Nuclear Studies and University of Warsaw, Ul. Hoza 69, PL-00681 Warsaw, Poland
[54]Fachbereich Physik, University of Wuppertal, Postfach 100 127, DE-42097 Wuppertal, Germany

1 Introduction

In 1999, the centre-of-mass energies reached by LEP ranged from 192 GeV to 202 GeV, and the DELPHI experiment collected an integrated luminosity of 228.2 pb^{-1}. These data were analysed to update the searches for sleptons, neutralinos and charginos in the context of Gauge Mediated Supersymmetry Breaking (GMSB) models [1,2] already performed at lower energies.

In these models the gravitino, $\tilde{G}$, is the lightest supersymmetric particle (LSP) and the next-to-lightest supersymmetric particle (NLSP) can be either the neutralino, $\tilde{\chi}_1^0$, or the sleptons, $\tilde{l}$ [3,4,5,6,7]. The data were analysed under the assumption that the NLSP is a slepton. Depending on the magnitude of the mixing between the left and right gauge eigenstates, $\tilde{\tau}_R$ and $\tilde{\tau}_L$, there are two possible scenarios. If the mixing is large†, $\tilde{\tau}_1$ (the lighter mass eigenstate) is the NLSP. However, if the mixing is negligible, $\tilde{\tau}_1$ is mainly right-handed [8] and almost mass degenerate with the other sleptons. In this case, the $\tilde{e}_R$ and $\tilde{\mu}_R$ three body decay ($\tilde{l} \rightarrow \tilde{\tau}_1 \tau l$ with $\tilde{\tau}_1 \rightarrow \tau \tilde{G}$), is very suppressed, and $\tilde{e}_R$ and $\tilde{\mu}_R$ decay directly into $l\tilde{G}$. This scenario is called sleptons co-NLSP.

Due to the coupling of the NLSP to $\tilde{G}$, the mean decay length, L, of the NLSP can range from micrometres to metres depending on the mass of the gravitino [9] ($m_{\tilde{G}}$):

$$L = 1.76 \times 10^{-3} \sqrt{\left(\frac{E_{\tilde{l}}}{m_{\tilde{l}}}\right)^2 - 1} \left(\frac{m_{\tilde{l}}}{100\,\text{GeV}/c^2}\right)^{-5} \left(\frac{m_{\tilde{G}}}{1\,\text{eV}/c^2}\right)^2 \text{ cm} \qquad (1)$$

For example, for $m_{\tilde{G}} \lesssim 250$ eV/c^2, or equivalently, for a SUSY breaking scale of $\sqrt{F} \lesssim 1000$ TeV (since both parameters are related [10]), the decay of a NLSP with mass greater than for example 60 GeV/c^2 can take place within the detector. This range of $\sqrt{F}$ is in fact consistent with astrophysical and cosmological considerations [11,12].

In this work the results of the searches reported in [13] are updated and the search for charginos is extended to the sleptons co-NLSP scenario. Moreover, the update of the search for heavy stable charged particles presented in [14] is also performed. Heavy stable charged particles are predicted not only in GMSB models but also in Minimal Supersymmetric Standard Models (MSSM) with a very small amount of R-parity violation, or with R-parity conservation if the mass difference between the LSP and the NLSP becomes very small. In these models the LSP can be a charged slepton or a squark and decay with a long lifetime into Standard Model particles [15]. Therefore, updated lower mass limits on heavy stable charged particles, under the assumption that the LSP is a charged slepton, will be provided in this letter within both models, GMSB and MSSM.

The first search looks for the production of $\tilde{\chi}_1^0$ pairs in the $\tilde{\tau}_1$ NLSP scenario

$$e^+e^- \rightarrow \tilde{\chi}_1^0 \tilde{\chi}_1^0 \rightarrow \tilde{\tau}_1^+ \tau^- \tilde{\tau}_1^+ \tau^- \rightarrow \tau^+ \tilde{G} \tau^- \tau^+ \tilde{G} \tau^- \qquad (2)$$

and in the sleptons co-NLSP scenario

$$e^+e^- \rightarrow \tilde{\chi}_1^0 \tilde{\chi}_1^0 \rightarrow \tilde{l}_R^+ l^- \tilde{l}_R'^+ l'^- \rightarrow l^+ \tilde{G} l^- l'^+ \tilde{G} l'^- \qquad (3)$$

with $l = e,\ \mu,\ \tau$ and BR($\tilde{\chi}_1^0 \rightarrow \tilde{l}l$) = 1/3 for each leptonic flavour. In the former case, neutralino pair production would mainly lead to a final state with four tau leptons and two gravitinos, while in the case of a co-NLSP scenario, the final signature would contain two pairs of leptons with possibly different flavour and two gravitinos.

---

†In GMSB models large mixing occurs generally in regions of $\tan\beta \geq 10$ (the ratio of the vacuum expectation values of the two Higgs doublets) or $|\mu| > 500$ GeV/c^2 (μ is the Higgs mass parameter).

The second search concerns $\tilde{l}$ pair production followed by the decay of each slepton into a lepton and a gravitino:

$$e^+e^- \rightarrow \tilde{l}^+\tilde{l}^- \rightarrow l^+\tilde{G}l^-\tilde{G} \tag{4}$$

This search has been performed within the $\tilde{\tau}_1$ NLSP scenario $(\tilde{l} = \tilde{\tau}_1)$ and the sleptons co-NLSP scenario $(\tilde{l} = \tilde{l}_R)$. The signature of these events will depend on the mean decay length of the NLSP, or equivalently, on the gravitino mass. Therefore, if the decay length is too short $(1 \text{ eV}/c^2 \lesssim m_{\tilde{G}} \lesssim 10 \text{ eV}/c^2)$ to allow the reconstruction of the slepton, only the corresponding lepton or its decay products will be seen in the detector, and the search will then be based on the track impact parameter. If the slepton decays inside the tracking devices $(10 \text{ eV}/c^2 \lesssim m_{\tilde{G}} \lesssim 1000 \text{ eV}/c^2)$, the signature will be at least one track of a charged particle with a kink or a decay vertex. However, for very heavy gravitinos $(m_{\tilde{G}} \gtrsim 1000 \text{ eV}/c^2)$, the decay length is large and the slepton decays outside the detector. The pair production of such long-lived or stable particles yields a characteristic signature with typically two back-to-back charged heavy objects in the detector. Finally, for very light gravitino masses $(m_{\tilde{G}} \lesssim 1 \text{ eV}/c^2)$, the decay takes place in the primary vertex and the results from the search for sleptons in gravity mediated (MSUGRA) models can be applied [16].

In the parameter space where the sleptons are the NLSP, there are specific regions where the chargino is light enough to be produced at LEP [5]. Therefore, the third search looks for the pair production of lightest charginos in the $\tilde{\tau}_1$ NLSP scenario

$$e^+e^- \rightarrow \tilde{\chi}_1^+\tilde{\chi}_1^- \rightarrow \tilde{\tau}_1^+\nu_\tau\tilde{\tau}_1^-\overline{\nu}_\tau \rightarrow \tau^+\tilde{G}\nu_\tau\tau^-\tilde{G}\overline{\nu}_\tau \tag{5}$$

and sleptons co-NLSP scenario

$$e^+e^- \rightarrow \tilde{\chi}_1^+\tilde{\chi}_1^- \rightarrow \tilde{l}_R^+\nu_l\tilde{l'}_R^-\overline{\nu}_{l'} \rightarrow l^+\tilde{G}\nu_l l'^-\tilde{G}\overline{\nu}_{l'}. \tag{6}$$

The analysis is divided into four topologies according to the mean lifetime of the slepton as explained in the previous paragraph: two acoplanar leptons with respect to the beam pipe with missing energy (MSUGRA models), at least one track with large impact parameter or a kink, or at least one track corresponding to a very massive stable charged particle.

The data samples are described in section 2. The efficiencies of the different selection criteria and the number of events selected in data and in the Standard Model background are reported in 3. Finally, the results are presented in section 4.

2 Data sample and event generators

All searches are based on data collected with the DELPHI detector during 1999 at centre-of-mass energies around 192, 196, 200 and 202 GeV. The total integrated luminosity was 228.2 pb^{-1}. A detailed description of the DELPHI detector can be found in [17] and the detector performance in [18].

To evaluate the signal efficiencies and background contamination, events were generated using different programs, all relying on JETSET 7.4 [19], tuned to LEP 1 data [20] for quark fragmentation.

The program SUSYGEN [21] was used to generate neutralino pair events and their subsequent decay products. In order to compute detection efficiencies, a total of 90000 events were generated with masses 67 GeV/$c^2 \leq m_{\tilde{\tau}_1} + 2$ GeV/$c^2 \leq m_{\tilde{\chi}_1^0} \leq \sqrt{s}/2$ and at the four centre-of-mass energies.

Slepton pair samples of 99000 and 76500 events at 196 GeV and 202 GeV centre-of-mass energies respectively were produced with PYTHIA 5.7[‡] [19] with staus having a mean decay length from 0.25 to 200 cm and masses from 40 to 100 GeV/c^2. Other samples of $\tilde{\tau}$ pairs were produced with SUSYGEN for the small impact parameter search with $m_{\tilde{\tau}}$ from 40 GeV/c^2 to 100 GeV/c^2.

For the search for heavy stable charged particles, signal efficiencies were estimated on the basis of about 50000 simulated events. Pair produced heavy smuons were generated at energies between 192 GeV and 202 GeV with SUSYGEN, and passed through the detector simulation as heavy muons. The efficiencies were estimated for masses between 10 GeV/c^2 and 97.5 GeV/c^2. 1000 events were generated per mass point.

SUSYGEN was also used to generate $\tilde{\chi}_1^{\pm}$ pair production samples and their decays at 192 GeV and 202 GeV centre-of-mass energies. In order to compute detection efficiencies, a total of 45 samples with 500 events each were generated with $m_{\tilde{G}}$ at 1, 100 and 1000 eV/c^2, $m_{\tilde{\tau}_1} + 0.3$ GeV/$c^2 \leq m_{\tilde{\chi}_1^+} \leq \sqrt{s}/2$ and $m_{\tilde{\tau}_1} \geq 65$ GeV/c^2. Samples with smaller $\Delta m = m_{\tilde{\chi}_1^+} - m_{\tilde{\tau}_1}$ were not generated because in this region the $\tilde{\chi}_1^{\pm}$ does not decay mainly to $\tilde{\tau}_1$ and ν_τ but into W and $\tilde{G}$.

The background process $e^+e^- \rightarrow q\bar{q}(n\gamma)$ was generated with PYTHIA 6.125, while KORALZ 4.2 [22] was used for $\mu^+\mu^-(\gamma)$ and $\tau^+\tau^-(\gamma)$. The generator BHWIDE [23] was used for $e^+e^- \rightarrow e^+e^-$ events.

Processes leading to four-fermion final states were generated using EXCALIBUR 1.08 [24] and GRC4F [25].

Two-photon interactions leading to hadronic final states were generated using TWOGAM [26], including the VDM, QPM and QCD components. The generators of Berends, Daverveldt and Kleiss [27] were used for the leptonic final states.

The cosmic radiation background was studied using the data collected before the beginning of the 1998 LEP run.

The generated signal and background events were passed through the detailed simulation [18] of the DELPHI detector and then processed with the same reconstruction and analysis programs used for real data.

3   Data selection

3.1   Neutralino pair production

The selection criteria used in the search for neutralino pair production in the $\tilde{\tau}_1$ NLSP scenario and in the sleptons co-NLSP scenario, were described in detail in [13,28]. The main two differences between these two cases are that the mean number of neutrinos carrying away undetected energy and momentum and the number of charged particles per event are considerably bigger for the $\tilde{\tau}_1$ NLSP scenario.

After applying the selection criteria to the search for these topologies, six events passed the search for neutralino pair production in the $\tilde{\tau}_1$ NLSP scenario, with 3.36±0.98 Standard Model (SM) background events expected. Four events passed the search for neutralino pair production in the sleptons co-NLSP scenario, with 4.39±0.51 SM background events expected. Efficiencies between 20% and 44% were obtained for the signal events.

[‡]Another two samples of 1000 events with $m_{\tilde{\tau}} = 60$ GeV/c^2 and mean decay lengths of 5 and 50 cm, were generated using SUSYGEN to cross check with the PYTHIA results. The same efficiencies were found within a ±2% difference.

3.2 Slepton pair production

This section describes the update of the search for slepton pair production as a function of the mean decay length. The details of the selection criteria used to search for the topologies obtained when the NLSP decays inside the detector volume were described in [13,28,29]. Likewise, the selection criteria used to search for heavy stable charged particles were described in detail in [14,30]. The efficiencies were derived for different $\tilde{l}$ masses and decay lengths by applying the same selection to the simulated signal events.

3.2.1 Search for secondary vertices

This analysis exploits a feature of the $\tilde{l} \to l\tilde{G}$ topology when the slepton decays inside the tracking devices, namely, one or two tracks originating from the interaction point and at least one of them with a secondary vertex or a kink. After applying the selection criteria to search for this topology, two events in real data were found to satisfy all the requirements, while $0.79^{+0.28}_{-0.12}$ were expected from SM backgrounds. One event was compatible with a $\gamma\gamma \to \tau^+\tau^-$ with a hadronic interaction in the Inner detector. The other one was compatible with a $e^+e^- \to \tau^+\tau^-$ event where one of the electrons (a decay product of the τ), after radiating a photon, was reconstructed as two independent tracks.

The secondary vertex reconstruction procedure was sensitive to radial decay lengths, R, between 20 cm and 90 cm. The Vertex detector and the Inner detector were needed to reconstruct the $\tilde{\tau}$ and the Time Projection Chamber to reconstruct the decay products. The shape of the efficiency distribution was essentially flat as a function of R decreasing when the $\tilde{\tau}$ decayed near the outer surface of the Time Projection Chamber. The decrease was due to inefficiencies in the reconstruction of the tracks coming from the decay products of the τ. The search for events with secondary vertices had an efficiency of $(52.8\pm2.0)\%$ for $\tilde{\tau}$ with masses between 40 and 100 GeV/c^2, with a mean decay length of 50 cm.

The same selection criteria were applied to smuons and selectrons. The efficiency was $(56.5\pm2.0)\%$ for $m_{\tilde{\mu}_R}$ between 40 to 100 GeV/c^2, and for selectrons it was $(38.1\pm2.0)\%$ in the same range of masses. The efficiency for selectrons was lower than for staus or smuons due to an upper cut on total electromagnetic energy at the preselection level.

3.2.2 Large impact parameter search

To investigate the region of lower gravitino masses the previous search was extended to the case of sleptons with mean decay length between 0.25 cm and approximately 10 cm. In this case the $\tilde{l}$ is not reconstructed and only the l (or the decay products in the case of $\tilde{\tau}$) is detected. The impact parameter search was only applied to those events accepted by the same general requirements as in the search for secondary vertices, and not selected by the secondary vertex analysis.

The maximum efficiency was $(31.0\pm2.0)\%$ corresponding to a mean decay length of 2.5 cm. The efficiency decreased sharply for lower decay lengths due to the requirement on minimum impact parameter. For longer decay lengths, the appearance of reconstructed $\tilde{\tau}$ in combination with the cut on the maximum number of charged particles in the event caused the efficiency to decrease smoothly. This decrease is compensated by a

rising efficiency in the search for secondary vertices. For masses above 40 GeV/c^2 no dependence on the $\tilde{\tau}$ mass was found far from the kinematic limit.

The same selection was applied to smuons and selectrons. For smuons the efficiency increased to $(60.0\pm2.0)\%$ for a mean decay length of 2.5 cm and masses over 40 GeV/c^2 since the smuon always has a one-prong decay. For selectrons the efficiency was $(36.3\pm2.0)\%$ for the same mean decay length and range of masses.

Trigger efficiencies were studied simulating the DELPHI trigger response to the events selected by the vertex search and by the large impact parameter analysis, and were found to be around 99%.

Two events in the real data sample were selected, while $1.77^{+0.25}_{-0.21}$ were expected from SM backgrounds. Both events are compatible with $e^+e^- \rightarrow \tau^+\tau^-$ events where one of the electrons (a decay product of the τ), after radiating a photon, was reconstructed only by the Inner detector and Time Projection Chamber detectors giving a very large impact parameter track.

3.2.3 Small impact parameter search

The large impact parameter search can be extended further to mean decay lengths below 0.1 cm. Here only the main points of the analysis and some changes with respect to previous ones are recalled. In low multiplicity events two hemispheres were defined using the thrust axis. The highest momentum, good quality (Δp/p < 50%), particle tracks in each hemisphere were labelled leading tracks. The impact parameters from the beam spot, b_1 and b_2, of the leading tracks in the Rϕ plane were used to discriminate against SM backgrounds. The same selection criteria described in references [13,28] were applied. However, some extra selection was added in order to reduce the background from detector noise or failure.

In order to preserve the efficiency in the region of decay length $\gtrsim$ 10 cm, where the $\tilde{\tau}$ can be observed as a particle coming from the primary vertex and badly measured owing to its limited length, further requirements on the track quality were applied only to the leading track with the larger impact parameter. This particle was required to have a relative momentum error < 30% and the track to be measured at least either in the Time Projection Chamber or in all of the other three track detectors in the barrel (Vertex detector, Inner detector and Outer detector).

The efficiency of the search did not show any significant dependence on the $\tilde{\tau}$ mass for masses over 40 GeV/c^2 and it could be parameterized as a function of the $\tilde{\tau}$ decay length in the laboratory system. The maximum efficiency was $\sim$ 38% for a mean decay length of $\sim$ 2 cm; the efficiency dropped at small decay lengths ($\sim$ 10% at 0.6 mm).

The same selection criteria were used to search for smuons as reported in [13]. The maximum efficiency reached for the smuon search was $\sim$ 43% at $\sim$ 2 cm mean decay length. To search for selectrons, in order to increase efficiency, the cut $(E_1 + E_2) < 0.7\ E_{beam}$ (where E_1, E_2 are the electromagnetic energy deposits associated to the leading tracks) was not applied. The Bhabha events that survived the selection, when the previous rejection cut was not applied, were those where at least one of the electrons underwent a secondary interaction, thus acquiring a large impact parameter. However, it was found that in these cases the measured momentum of the electron was smaller than the electromagnetic energy deposition around the electron track. Therefore, the cut $(E_1/p_1 + E_2/p_2) < 2.2$ was used for the selectron search. The maximum efficiency reached in the selectron search was $\sim$ 35% at $\sim$ 2 cm mean decay length.

Requiring $\sqrt{b_1^2 + b_2^2} > 600$ μm, the number of events selected in the data was 5 in the $\tilde{\tau}$ and $\tilde{\mu}$ search, and 4 in the $\tilde{e}$ search, while 5.05±0.39 events were expected from the SM background in both searches. All of the selected candidates were compatible with SM events.

3.2.4 Heavy stable charged particle search

The analysis described in [14] has been applied for each of the four centre-of-mass energies 192, 196, 200 and 202 GeV. A careful run selection ensured that the Ring Imaging CHerenkov (RICH) detectors were fully operational because the method used to identify heavy stable particles relies on the lack of Cherenkov radiation in DELPHI's RICH detectors. The luminosities analysed after the run selection are shown in Table 1. Signal efficiencies were estimated from Monte Carlo by simulating heavy sleptons with `SUSYGEN` and passing them through the detector simulation as heavy muons. The background given in Table 1 was estimated from data itself by counting the number of tracks passing the individual selection criteria. Only events with two or three charged particles were considered. Events were selected, if they contained at least one charged particle with:

1. a momentum above 5 GeV/c, a high ionization loss and no photons in the gas radiator were associated to the particle (gas veto) or,
2. a momentum above 15 GeV/c, an ionization loss at least 0.3 below the expectation for a proton and surviving the gas veto or,
3. a momentum above 15 GeV/c, surviving the gas and the liquid RICH veto.

An event was also selected if both event hemispheres contained particles with both either a high ionization loss or a gas veto, or both having a low ionization loss.

No candidate events were selected in data. As an example, Figure 1 show the data and the three main search windows for the search at an energy of 202 GeV. The expectation for a 90 GeV/c^2 mass signal is also shown. For particle masses below 60 GeV/c^2 the signal efficiencies are of the order of 30%, and rise with increasing mass to about 78%. Then the efficiency drops when approaching the kinematical limit due to saturation effects, and it is assumed to be zero at the kinematical limit.

$\sqrt{s}$	192 GeV	196 GeV	200 GeV	202 GeV
$\mathcal{L}$ (pb^{-1})	26.3	69.7	87.1	40.4
background	0.12±0.04	0.18±0.04	0.31±0.06	0.1±0.03
observed	0	0	0	0

Table 1: Luminosities analysed and selected events for each of the four centre-of-mass energies in the search for heavy stable charged particles.

3.3 Chargino pair production

The search for the lightest chargino depends on the slepton lifetime, or equivalently on the gravitino mass as already stated. For $m_{\tilde{G}} \lesssim 1$ eV/c^2, $\tilde{\chi}_1^\pm$ decays at the vertex and the final state is two acoplanar leptons with missing energy. In this case the search for charginos and for sleptons in gravity mediated scenarios (MSUGRA) can be applied. The details of the search for charginos in MSUGRA models can be found in [31]. The

efficiencies obtained using these analyses were 13-36% for the $\tilde{\tau}_1$ NLSP scenario and 15-29% for the sleptons co-NLSP scenario. The number of selected events in data was 39, while the background expected from SM was $37.58^{+2.02}_{-0.90}$ for the $\tilde{\tau}_1$ NLSP scenario. For the sleptons co-NLSP scenario the number of candidates in data was 81, while the number of events expected from SM was 79.7±3.9. For $m_{\tilde{G}}$ between 1 eV/c^2 and 1000 eV/c^2, $\tilde{\chi}^\pm_1$ has intermediate mean decay lengths and the final topologies are events with kinks or large impact parameter tracks. The efficiencies obtained with these analyses were 25-56% in the $\tilde{\tau}_1$ NLSP scenario, and 41-56% in the sleptons co-NLSP scenario. Four events in real data were found to satisfy all the conditions required in the search for charginos with intermediate mean decay lengths, while $2.56^{+0.38}_{-0.24}$ events were expected from SM backgrounds. These results apply to both scenarios $\tilde{\tau}_1$ NLSP and sleptons co-NLSP, since the same selection criteria were applied to search for staus, smuons and selectrons.

Finally, for $m_{\tilde{G}} > 1000$ eV/c^2 the event topology is at least one track corresponding to a very massive stable charged particle. Therefore the search for stable charged particles was applied. In this case the efficiency is mainly affected by the momentum of the slepton because the method used to identify heavy stable particles relies on the lack of Cherenkov radiation in DELPHI's RICH detectors as already stated in section 3.2.4. To remove SM backgrounds, low momentum particles are removed, thus reducing the efficiency for higher chargino masses, especially in the region where the mass difference (Δm) between the NLSP and the LSP is small. Therefore for this analysis the efficiencies vary from 0% for $\Delta m = 300$ MeV/c^2 to 62% for $\Delta m = 20$ GeV/c^2. No candidates in the data passed the selection cuts, while 0.71±0.09 events were expected from background.

4 Results and interpretation

Since there was no evidence for a signal above the expected background, the number of candidates in data and the expected number of background events were used to set limits at the 95% confidence level (CL) on the pair production cross-section and masses of the sparticles searched for. The model described in reference [4] was used to derive limits within the GMSB scenarios. This model assumes radiatively broken electroweak symmetry and null trilinear couplings at the messenger scale. The corresponding parameter space was scanned as follows: $1 \leq n \leq 4$, 5 TeV $\leq \Lambda \leq$ 90 TeV, $1.1 \leq M/\Lambda \leq 10^9$, $1.1 \leq \tan\beta \leq 50$, and $sign(\mu) = \pm 1$, where n is the number of messenger generations in the model, Λ is the ratio between the vacuum expectation values of the auxiliary component and the scalar component of the superfield and M is the messenger mass scale. The parameters $\tan\beta$ and μ are defined as for MSUGRA. The limits presented here are at $\sqrt{s} = 202$ GeV after combining the results of the searches at lower centre-of-mass energies with the likelihood ratio method [32].

4.1 Neutralino pair production

Limits for neutralino pair production cross-section were derived in the $\tilde{\tau}_1$ NLSP and sleptons co-NLSP scenarios for each ($m_{\tilde{\chi}^0_1}$,$m_{\tilde{l}}$) combination. For the $\tilde{\tau}_1$ NLSP case, the combination took into account the results from the LEP runs from 1996 (for $\sqrt{s} \geq 161$ GeV) to 1999. The limits for the production cross-section allowed some sectors of the ($m_{\tilde{\chi}^0_1}, m_{\tilde{l}}$) space to be excluded. In order to exclude as much as possible of the mass plane, the results from two other analyses were taken into account. The first is the search for slepton pair production in the context of MSUGRA models. In the case where the MSUGRA $\tilde{\chi}^0_1$ is massless, the kinematics correspond to the case of $\tilde{l}$ decaying into a

lepton and a gravitino. The second is the search for lightest neutralino pair production in the region of the mass space where $\tilde{\chi}_1^0$ is the NLSP [33] (the region above the diagonal line in Figure 2, i.e. $m_{\tilde{\tau}_1} > m_{\tilde{\chi}_1^0}$). Within this zone, the neutralino decays into a gravitino and a photon.

As an illustration, Figure 2 presents the 95% CL excluded areas for $m_{\tilde{G}} < 1$ eV/c^2 in the $m_{\tilde{\chi}_1^0}$ vs $m_{\tilde{\tau}_1}$ plane for the $\tilde{\tau}_1$ NLSP. The negative-slope dashed area is excluded by the analysis searching for neutralino pair production followed by the decay $\tilde{\chi}_1^0 \to \tilde{G}\gamma$. The point-hatched area is excluded by the direct search for slepton pair production within MSUGRA scenarios.

4.2   Slepton pair production

The results of the search for slepton pair production are presented in the $(m_{\tilde{G}}, m_{\tilde{l}})$ plane combining the two impact parameter searches, the secondary vertex analysis and the stable heavy lepton search, and using all DELPHI data from 130 GeV to 202 GeV centre-of-mass energies.

The $\tilde{\tau}_1$ pair production cross-section depends on the mixing in the stau sector. Therefore, in order to put limits on the $\tilde{\tau}_1$ mass the mixing angle had to be fixed. The results presented here correspond to the case when there is no mixing between the $\tilde{\tau}_R$ and $\tilde{\tau}_L$, thus $\tilde{\tau}_1$ is a pure right-handed state (Figure 3-a). In the case which corresponds to a mixing angle which gives the minimum $\tilde{\tau}_1$ pair production cross-section and at the same time maintains $m_{\tilde{\tau}_1}^2 > 0$, the given limit was reduced by ~ 1 GeV. Therefore, within the $\tilde{\tau}_1$ NLSP scenario, the impact parameter and secondary vertex analyses extended the limit $m_{\tilde{\tau}_R} > 75$ GeV/c^2 for $m_{\tilde{G}} \lesssim 1$ eV/c^2, set by MSUGRA searches [16], up to $m_{\tilde{G}} = 400$ eV/c^2, reaching the maximum excluded value of $m_{\tilde{\tau}_R} = 92$ GeV/c^2 for $m_{\tilde{G}} = 200$ eV/c^2. For $m_{\tilde{G}} > 250$ eV/c^2 the best lower mass limit was set by the stable heavy lepton search.

Within the sleptons co-NLSP scenario, the cross-section limits were used to derive lower limits for $\tilde{\mu}_R$ (Figure 3-b) and $\tilde{e}_R$ (Figure 3-c) masses at 95% CL. The $\tilde{\mu}_R$ pair production cross-section is model independent, however, the $\tilde{e}_R$ pair production cross-section is a function of the GMSB parameters due to the exchange of a $\tilde{\chi}_1^0$ in the t–channel. Therefore, in order to put limits on the $\tilde{e}_R$ mass, the aforementioned region of the GMSB parameter space was scanned and, for each selectron mass, the smallest theoretical production cross-section was chosen for comparison with the experimental limits. For gravitino masses below a few eV/c^2, the experimental limits are the ones corresponding to the search for selectrons in MSUGRA models.

Assuming mass degeneracy between the sleptons, (Figure 3-d), these searches extended the limit $\tilde{l}_R > 80$ GeV/c^2 set by MSUGRA searches [16] for very short NLSP lifetimes, up to $m_{\tilde{G}} = 700$ eV/c^2. For the MSUGRA case no lepton combination exists, so the best limit from the $\tilde{\mu}_R$ has been used. The maximum excluded value of $m_{\tilde{l}_R} = 94$ GeV/c^2 was achieved for $m_{\tilde{G}} = 200$ eV/c^2. For $m_{\tilde{G}} > 700$ eV/c^2 the best lower mass limit was set by the stable heavy lepton search. $\tilde{l}_R$ masses below 35 GeV/c^2 were excluded by LEP 1 data [34]. In the case of $\tilde{l}_R$ degeneracy, this limit improved to 41 GeV/c^2.

4.3   Chargino pair production

The limits on the chargino pair production cross-section were used to exclude areas within the $(m_{\tilde{\chi}_1^+}, m_{\tilde{l}})$ plane for different domains of the gravitino mass combining results from all the centre-of-mass energies from 183 GeV to 202 GeV. Figure 4 shows the

regions excluded at 95% CL in the $(m_{\tilde{\chi}_1^+}, m_{\tilde{\tau}_1})$ plane (a) and $(m_{\tilde{\chi}_1^+}, m_{\tilde{l}_R})$ plane (b). The positive-slope area is excluded for all gravitino masses. The negative-slope area is only excluded for $m_{\tilde{G}} \gtrsim 100$ eV/c^2 and the brick area for $m_{\tilde{G}} \gtrsim 1$ keV/c^2. The areas below $m_{\tilde{\tau}_1} = 73$ GeV/c^2 (Figure 4 (a)) and below $m_{\tilde{l}_R} = 80$ GeV/c^2 (Figure 4 (b)), are excluded by the direct search for slepton pair production in MSUGRA models [16]. The area of $\Delta m \leq 0.3$ GeV/c^2 is not excluded because in this region the charginos do not decay mainly to $\tilde{\tau}_1$ and ν_τ, but to W and $\tilde{G}$. Thus, if $\Delta m \geq 0.3$ GeV/c^2, the chargino mass limits are 95.2, 96.8 and 99 GeV/c^2 for $m_{\tilde{G}} = 1$, 100 and 1000 eV/c^2 respectively, in the $\tilde{\tau}_1$ NLSP scenario. In the sleptons co-NLSP scenario the limits are 95.2, 98.6 and 98.6 GeV/c^2 for $m_{\tilde{G}} = 1$, 100 and 1000 eV/c^2 respectively. The limit at $m_{\tilde{G}} = 1$ eV/c^2 is also valid for smaller masses of the gravitino, because they lead to the same final state topologies. The same argument is true for $m_{\tilde{G}} \gtrsim 1$ keV/c^2. The chargino mass limit decreases with decreasing $m_{\tilde{\tau}_1}$ because in scenarios with gravitino LSP, small stau masses correspond to small sneutrino masses (both are proportional to Λ) and hence to smaller production cross-sections due to the destructive interference between the s- and t-channels. It should be noticed that within the parameter space covered by this work, the lightest chargino is at least 40% heavier than the lightest neutralino. Thus, for gravitino masses up to ~ 1 eV/c^2 the search for neutralinos implies a model dependent lower limit on the lightest chargino of 125 GeV/c^2. However, neutralinos were not directly searched for in heavier gravitino mass regions, therefore, a model dependent lower limit cannot be set in this case. Thus, the experimental lower limit of 98.6 GeV/c^2 remains valid.

4.4   Heavy stable charged particle pair production

The results presented in section 3.2.4 were combined with previous DELPHI results in this channel, and cross-section limits were derived as indicated in Figure 5. From the intersection points with the predicted cross-sections for smuon or staus in the MSSM, left(right) handed smuons and staus can be excluded up to masses of 94.0(93.5) GeV/c^2 at 95%CL. No limits are given on selectrons here, because the cross-section can be highly suppressed by an additional t-channel sneutrino exchange contribution.

4.5   Limits on the GMSB parameter space

Finally, all these results can be combined to produce exclusion plots within the $(\tan\beta, \Lambda)$ space. The corresponding parameter space was scanned as follows: $1 \leq n \leq 4$, 5 TeV $\leq \Lambda \leq 90$ TeV, $1.1 \leq M/\Lambda \leq 10^9$, $1.1 \leq \tan\beta \leq 50$, and $sign(\mu) = \pm 1$. As an example, Figure 6 shows the zones excluded for $n =1$ to 4 for $m_{\tilde{G}} \leq 1$ eV/c^2, which corresponds to the NLSP decaying at the main vertex. The shaded areas are excluded. The areas below the dashed lines contain points of the GMSB parameter space with $\tilde{\chi}_1^0$ NLSP. The areas to the right (above for $n = 1$) of the dashed-dotted lines contain points of the GMSB parameter space where sleptons are the NLSP. It can be seen that the region of slepton NLSP increases with n. The contrary occurs to the region of neutralino NLSP. A limit could be set for the variable Λ at 17.5 TeV.

5   Summary

Lightest neutralino, slepton and chargino pair production were searched for in the context of light gravitino models. Two possibilities were explored: the $\tilde{\tau}_1$ NLSP and the sleptons co-NLSP scenarios. No evidence for signal production was found. Hence, the

DELPHI collaboration sets lower limits at 95% CL for the mass of the $\tilde{\chi}_1^0$ at 86 GeV/c^2 if $m_{\tilde{G}} \lesssim 1$ eV/c^2, and lower mass limits for the sleptons in all the gravitino mass range. The limit on the chargino mass is 95.2 GeV/c^2 for all $m_{\tilde{G}}$ in both scenarios, $\tilde{\tau}_1$ NLSP and the sleptons co-NLSP.

Finally, mass limits for heavy stable charged particles were also derived within the MSSM. For these particles the DELPHI collaboration sets lower mass limits at 95% CL for the left (right) handed sleptons at 94.0 (93.5) GeV/c^2.

Acknowledgements

References

[1] M. Dine, W. Fischler and M. Srednicki, Nucl. Phys. **B189** (1981) 575;
S. Dimopoulos and S. Raby, Nucl. Phys. **B192** (1981) 353;
M. Dine and W. Fischler, Phys. Lett. **B110** (1982) 227;
M. Dine and M. Srednicki, Nucl. Phys. **B202** (1982) 238;
L. Alvarez-Gaumé, M. Claudson and M. Wise, Nucl. Phys. **B207** (1982) 96;
C. Nappi and B. Ovrut, Phys. Lett. **B113** (1982) 175.

[2] M. Dine and W. Fischler, Nucl. Phys. **B204** (1982) 346;
S. Dimopoulos and S. Raby, Nucl. Phys. **B219** (1983) 479.

[3] J. A. Bagger, K. Matchev, D. M. Pierce and R. Zhang, Phys. Rev. **D55** (1997) 3188.

[4] D. A. Dicus, B. Dutta, S. Nandi, Phys. Rev. **D56** (1997) 5748;
D. A. Dicus, B. Dutta, S. Nandi, Phys. Rev. Lett. **78** (1997) 3055.

[5] K. Cheung, D. A. Dicus, B. Dutta, S. Nandi, Phys. Rev. **D58** (1998) 015008.

[6] F. Borzumati, hep-ph/9702307 and WIS/96-50-PH, Dec. 1996.

[7] G. F. Giudice, R. Rattazzi, Phys. Rep. 322 (1999) 419.

[8] A. Bartl *et. al.*, Z. Phys. **C73** (1997) 469.

[9] S. P. Martin, hep-ph/9709356.

[10] S. Deser and B. Zumino, *Phys. Rev. Lett.* **38** (1977) 1433;
E. Cremmer et al., *Phys. Lett.* **B 79** (1978) 231.

[11] S. Dimopoulos, M. Dine, S. Raby, S. Thomas and J. D. Wells, Nucl. Phys. Proc. Suppl. **A52** (1997) 38.

[12] E. Calzetta, A. Kandus, F. D. Mazzitelli and C. E. M. Wagner, Phys. Lett. **B472** (2000) 287.

[13] DELPHI Collaboration, P. Abreu *et al.*, Eur. Phys. J. **C16** (2000) 211.

[14] DELPHI Collaboration, P. Abreu *et al.*, Phys. Lett. **B478** (2000) 65.

[15] H. Dreiner, hep-ph/9707435.

[16] DELPHI Collaboration, P. Abreu *et al.*, CERN EP 2000-134, to be published on Eur. Phys. J**C**.

[17] DELPHI Collaboration, P. Aarnio *et al.*, Nucl. Instr. and Meth. **303** (1991) 233.

[18] DELPHI Collaboration, P. Abreu *et al.*, Nucl. Instr. and Meth. **378** (1996) 57.

[19] T. Sjöstrand, Comp. Phys. Comm. **39** (1986) 347;
T. Sjöstrand, `PYTHIA 5.6` *and* `JETSET 7.3`, CERN-TH/6488-92.

[20] DELPHI Collaboration, P. Abreu *et al.*, Z. Phys. **C73** (1996) 11.

[21] SUSYGEN 2.20, S. Katsanevas and S. Melachroinos in *Physics at LEP2*, CERN 96-01, **Vol. 2**, p. 328 and http://lyoinfo.in2p3.fr/susygen/susygen.html;
S. Katsanevas and P. Moravitz, Comp. Phys. Comm. **122** (1998) 227.

[22] S. Jadach, B.F.L. Ward and Z. Was, Comp. Phys. Comm. **79** (1994) 503.

[23] S. Jadach, W. Placzek, B.F.L. Ward, Phys. Lett. **B390** (1997) 298.

[24] F.A. Berends, R. Pittau, R. Kleiss, Comp. Phys. Comm. **85** (1995) 437.

[25] J. Fujimoto *et al.*, Comp. Phys. Comm. **100** (1997) 128.

[26] S. Nova, A. Olshevski, and T. Todorov, CERN Report 96-01, Vol. 2, p 224.

[27] F.A. Berends, P.H. Daverveldt, R. Kleiss, Comp. Phys. Comm. **40** (1986) 271,
Comp. Phys. Comm. **40** (1986) 285, Comp. Phys. Comm. **40** (1986) 309.

[28] DELPHI Collaboration, P. Abreu *et al.*, Eur. Phys. J. **C7** (1999) 595.

[29] DELPHI Collaboration, P. Abreu *et al.*, Eur. Phys. J. **C6** (1999) 385.

[30] DELPHI Collaboration, P. Abreu *et al.*, Phys. Lett. **B444** (1998) 491.

[31] DELPHI Collaboration, P. Abreu *et al.*, Phys. Lett. **B479** (2000) 118;
DELPHI Collaboration, P. Abreu *et al.*, Phys. Lett. **B446** (1999) 75.

[32] A.L. Read, *Modified Frequentist Analysis of Search Results (The CLs Method)*, CERN 2000-205.

[33] DELPHI Collaboration, P. Abreu *et al.*, Eur. Phys. J. **C17** (2000) 53;
DELPHI Collaboration, P. Abreu *et al.*, Eur. Phys. J. **C6** (1999) 371;

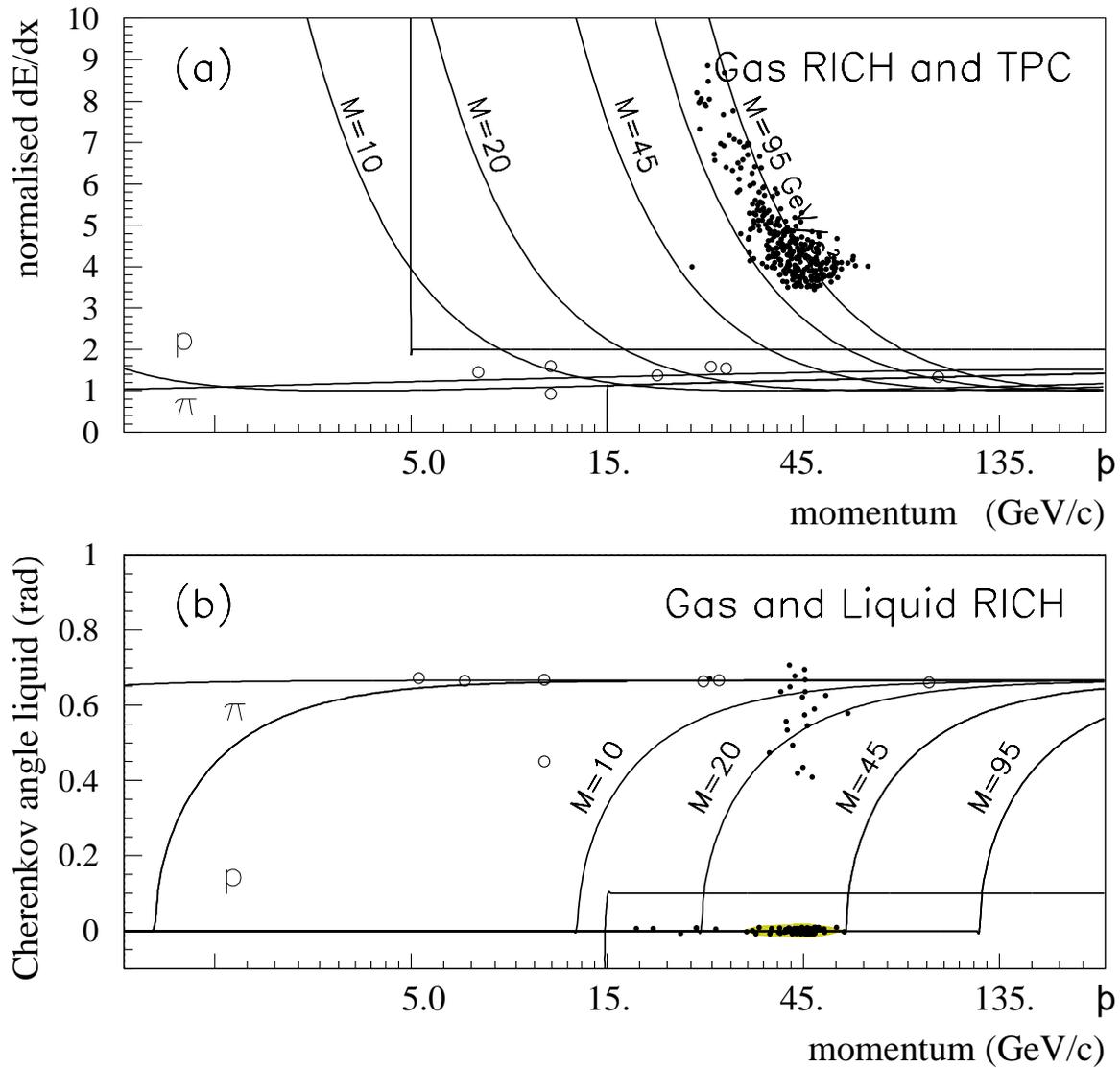[34] Particle Data Group, Eur. Phys. J. **C15** (2000) 1.

Figure 1:   (a) Normalised energy loss as a function of the momentum after the gas veto for the 202 GeV data. (b) Measured Cherenkov angle in the liquid radiator as a function of the momentum after the gas veto: if four photons or less were observed in the liquid radiator, the Cherenkov angle was set equal to zero. The rectangular areas in (a) indicate selections (1) and (2), and that in (b) shows selection (3). The selection criteria are explained in the text. Open circles are data. The small filled circles indicate the expectation for a 90 GeV/c^2 mass signal with charge $\pm$e, resulting in a large dE/dx (upper plot) and no photons (except for a few accidental rings) in the liquid Cherenkov counter (lower plot). The solid lines with a mass signal value indicate the expectation for heavy stable sleptons.
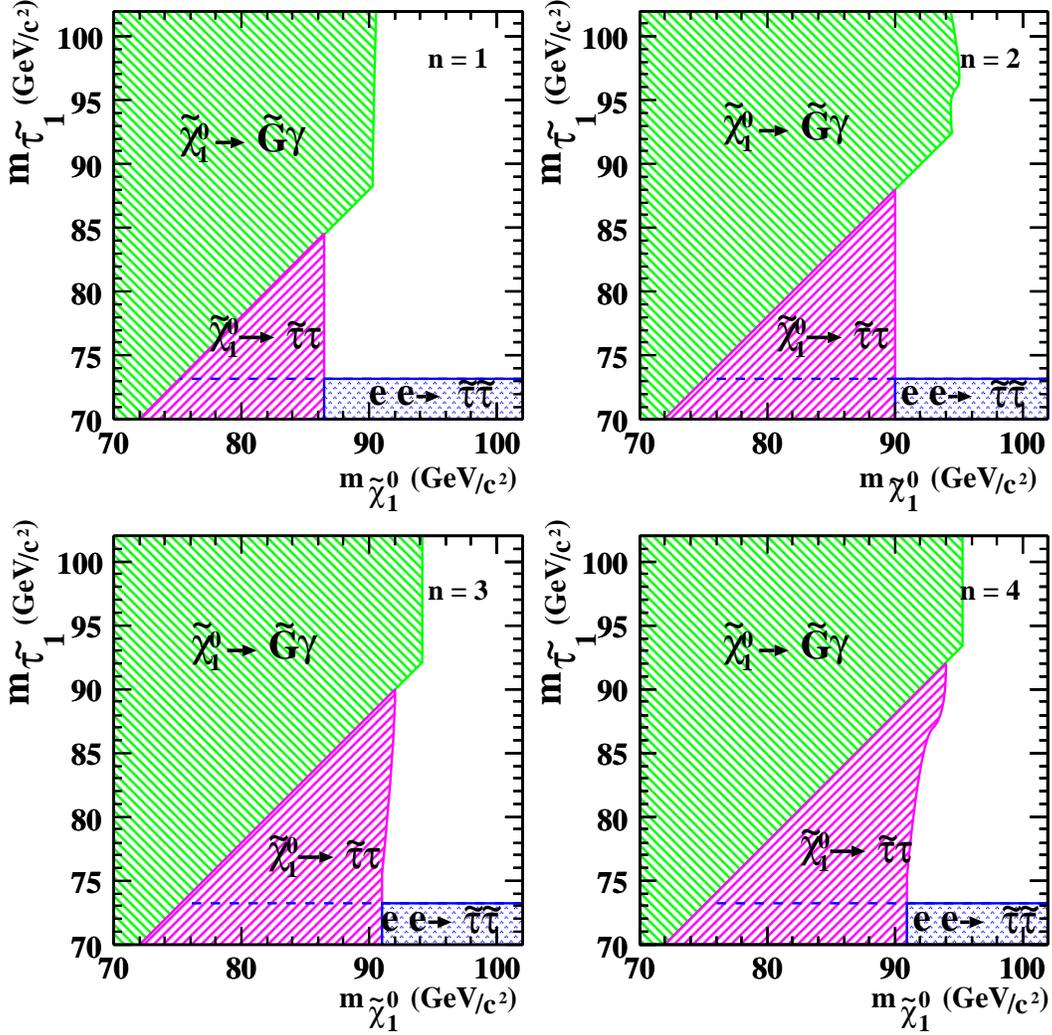
Figure 2: Areas excluded at 95% CL with $m_{\tilde{G}} < 1$ eV/c^2 in the $m_{\tilde{\chi}_1^0}$ vs $m_{\tilde{\tau}_1}$ plane for $n = 1$ to 4, using all data from 161 GeV to 202 GeV centre-of-mass energies. The positive-slope dashed area is excluded by this analysis. The negative-slope dashed area is excluded by the search for $\tilde{\chi}_1^0 \to \gamma\tilde{G}$, and the point-hatched area by the direct search for stau pair production in the MSUGRA framework.
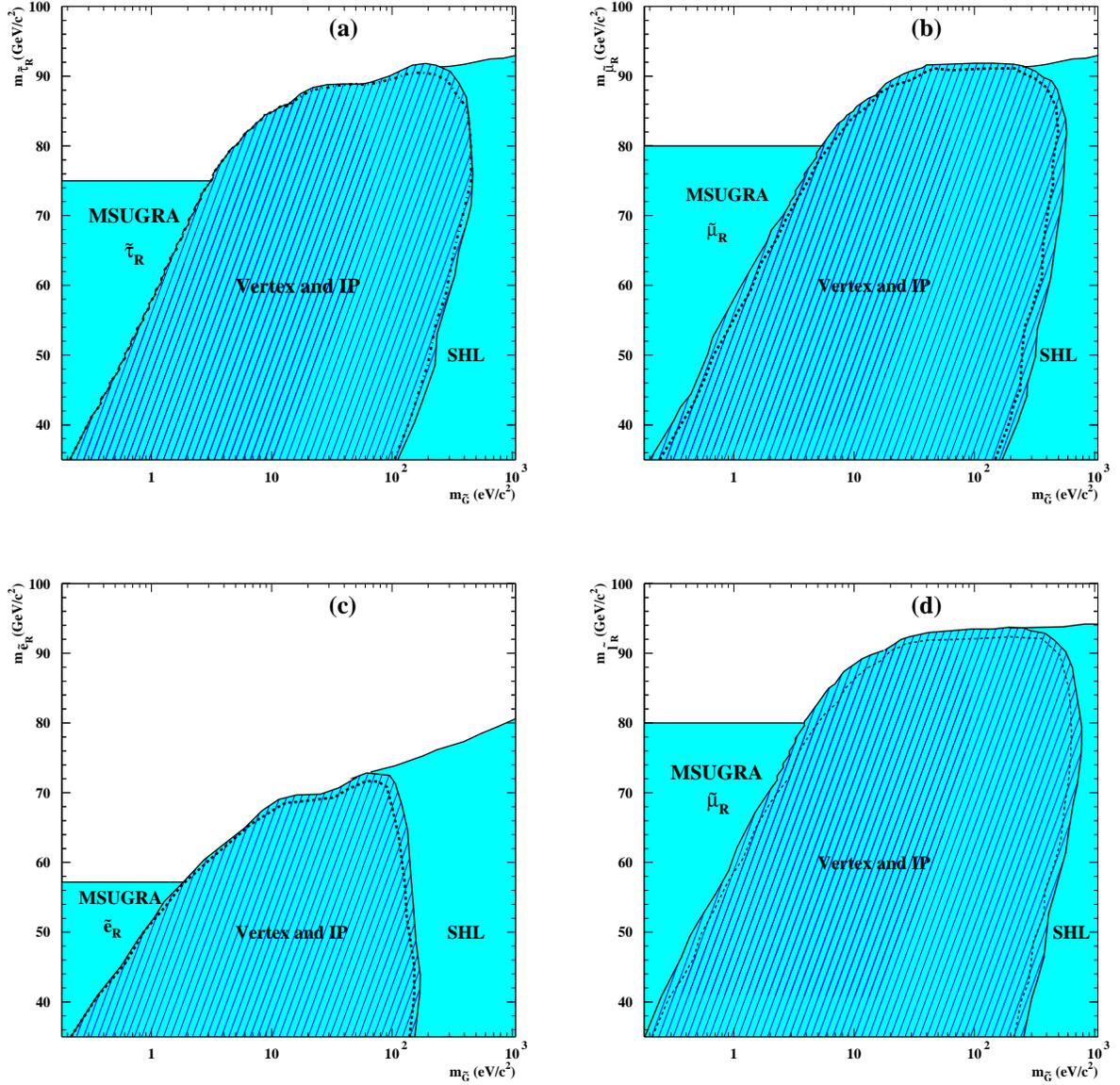
Figure 3: Exclusion regions in the $(m_{\tilde{G}},m_{\tilde{\tau}_R})$ (a), $(m_{\tilde{G}},m_{\tilde{\mu}_R})$ (b), $(m_{\tilde{G}},m_{\tilde{e}_R})$ (c) $(m_{\tilde{G}},m_{\tilde{l}_R})$ (d) planes at 95% CL for the present analyses combined with the Stable Heavy Lepton (SHL) search and the search for $\tilde{l}$ in gravity mediated models (MSUGRA), using all DELPHI data from 130 GeV to 202 GeV centre-of-mass energies. The positive-slope hatched area shows the region excluded by the combination of the impact parameter and secondary vertex searches. The dashed line shows the expected limits.
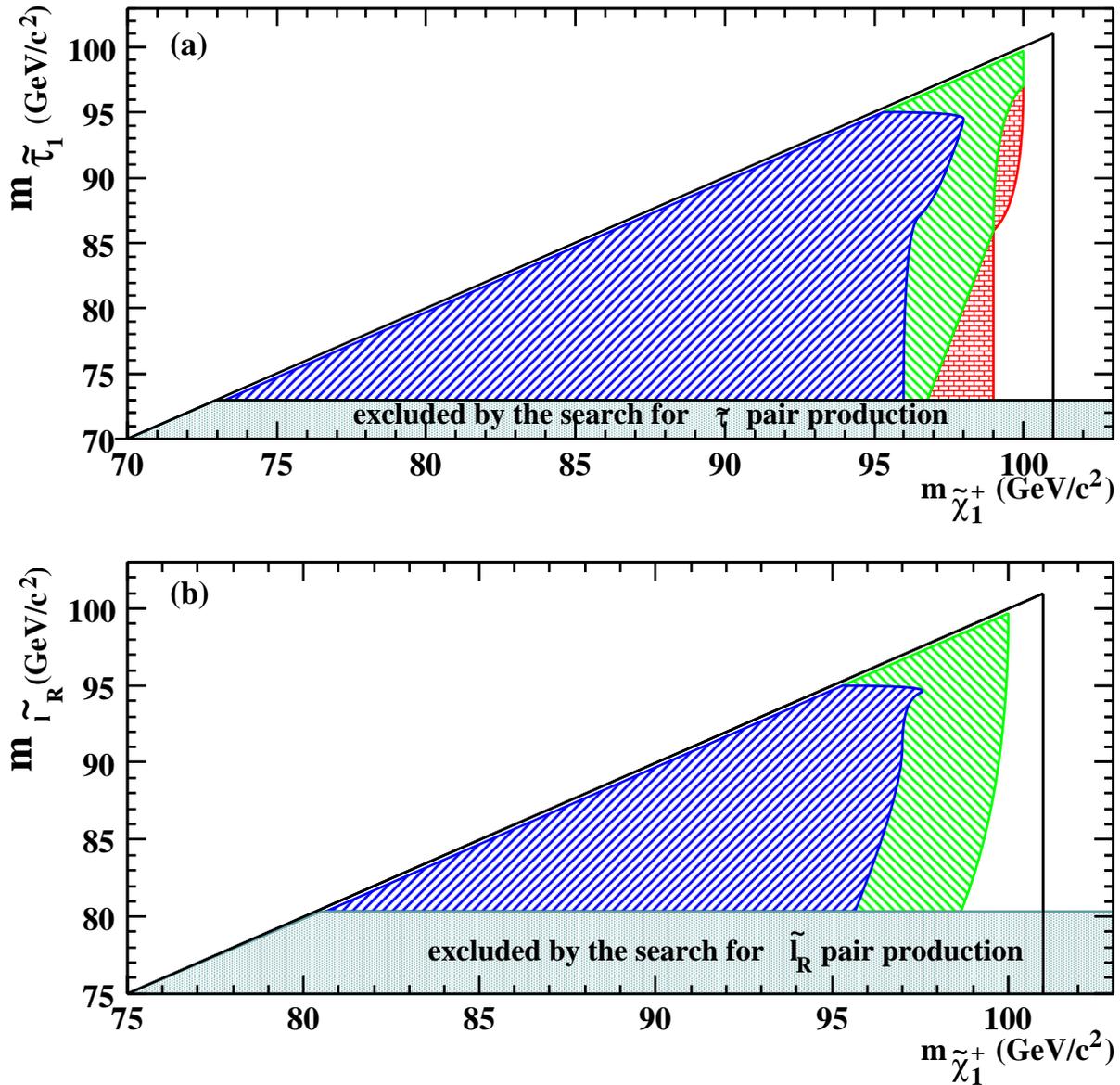
Figure 4: Areas excluded at 95% CL in the $(m_{\tilde{\chi}_1^+}, m_{\tilde{\tau}_1})$ plane (a) and $(m_{\tilde{\chi}_1^+}, m_{\tilde{l}_R})$ plane (b) using all DELPHI data from 183 GeV to 202 GeV centre-of-mass energies. The positive-slope area is excluded for all $m_{\tilde{G}}$. The negative-slope area is excluded only for $m_{\tilde{G}} \geq 100$ eV/c^2 and the brick area for $m_{\tilde{G}} \gtrsim 1$ keV/c^2. The grey area is excluded by the direct search for slepton pair production within MSUGRA models.
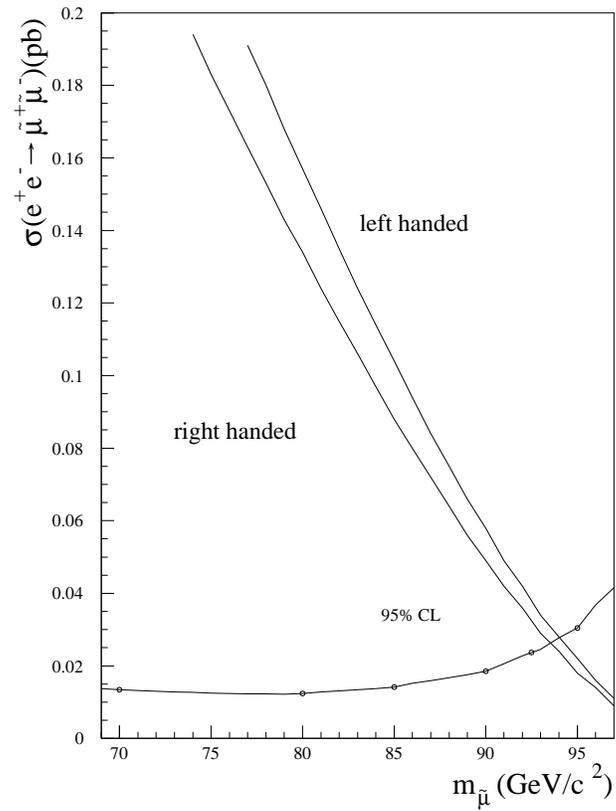
Figure 5: Predicted production cross-section for left and right handed stable smuons (staus) as a function of the particle mass. The cross-section limit indicated in the figure has been derived using all DELPHI data between 130 and 202 GeV.
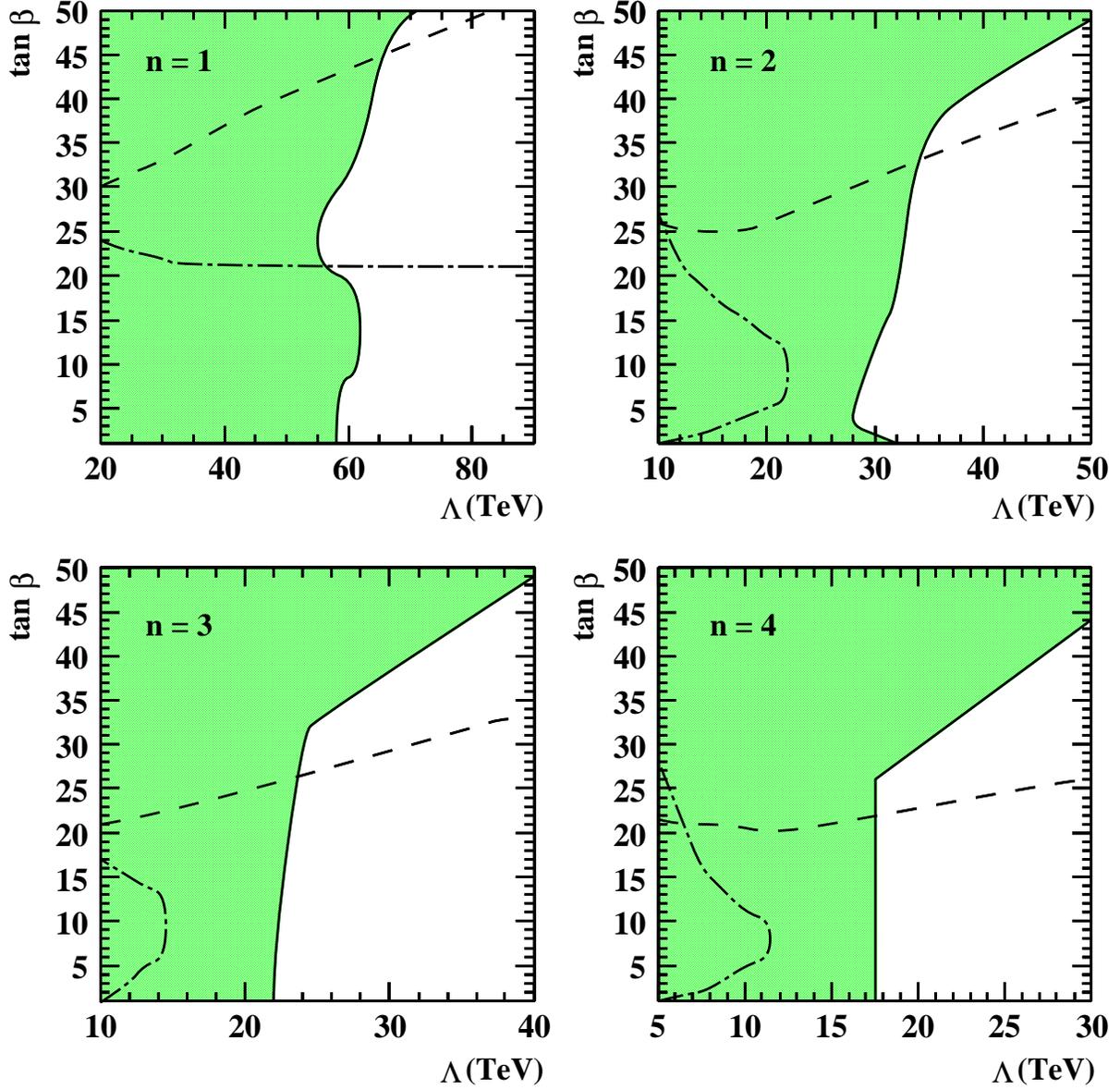
Figure 6: Shaded areas in the $(\tan\beta, \Lambda)$ plane are excluded at 95% CL. The areas below the dashed lines contain points of the GMSB parameter space with $\tilde{\chi}_1^0$ NLSP. The areas to the right (above for $n = 1$) of the dashed-dotted lines contain points of the GMSB parameter space were sleptons are the NLSP.